Available online at www.sciencedirect.com
SCIENCE DIRECT®
Journal of Sound and Vibration 287 (2005) 227–243
JOURNAL OF SOUND AND VIBRATION
www.elsevier.com/locate/jsvi

Sound absorption of a finite flexible micro-perforated panel backed by an air cavity

Y.Y. Lee[a,*], E.W.M. Lee[a], C.F. Ng[b]

[a]*Department of Building and Construction, City University of Hong Kong, 83 Tat Chee Avenue, Kowloon Tong, Kowloon, Hong Kong*
[b]*Department of Civil and Structural Engineering, Hong Kong Polytechnic University, Hung Hom, Kowloon, Hong Kong*

Received 26 April 2004; received in revised form 6 October 2004; accepted 2 November 2004
Available online 1 February 2005

Abstract

Micro-perforated absorbers have been studied for decades. In the experimental results of some previous works, an unexpected peak due to the flexible panel vibration effect was found on the absorption coefficient curve. In this paper, the acoustic absorption of a finite flexible micro-perforated panel backed by an air cavity is studied in detail. The absorption formula that is developed for the micro-perforated absorber is based on the modal analysis solution of the classical plate equation coupled with the acoustic wave equation. Another approach to derive a simpler absorption formula is also developed. The predictions from the two formulas are very close, except for those at the resonant frequencies of the higher structural modes and acoustic modes parallel to the panel surface. The theoretical results show good agreement with the measurements. It can be concluded that (1) as the panel vibration effect can dissipate more energy, the corresponding absorption peaks can widen the absorption bandwidth of a micro-perforated absorber by appropriately selecting the parameters such as panel thickness, perforation diameter, and perforation spacing, etc., such that the structural resonant frequency is higher than the absorption peak frequency caused by the perforations; (2) the comparison of the cases of different panel mode shapes does not show a significant difference in the absorption performance; and (3) the structural damping effect can improve the absorption performance at the frequencies between the structural resonant frequencies and the peak frequency of the micro-perforation effect, and decrease the peak absorption values of the structural resonances.

*Corresponding author. Fax: +852 27788 7612.
E-mail address: bcraylee@cityu.edu.hk (Y.Y. Lee).

0022-460X/$ - see front matter © 2004 Elsevier Ltd. All rights reserved.
doi:10.1016/j.jsv.2004.11.024

Nomenclature

a and b length and width of the perforated panel

A_{mn} modal amplitude of the (m,n) mode

$B_{mn} = \mathrm{i}\omega A_{mn}$ modal velocity amplitude of the (m,n) mode

c_a speed of sound

d perforation diameter

$D_p = \dfrac{Et^3}{12(1-\nu^2)}$ panel's flexural rigidity

E Young's modulus

f frequency (kHz)

L^{uw} and N^{uw} coefficients which depend on the boundary conditions at $z = 0$ and $-D$

$\ell_{m,n}$ and $\bar{\lambda}_{m,n}$ nth for a particular m solution of the equation
$\ell\bar{\lambda}(\cos(\ell b)\cosh(\bar{\lambda}b) - 1) + (\ell^2 - \bar{\lambda}^2)\sin(\ell b)\sinh(\bar{\lambda}b) = 0$

M and N numbers of structural modes used

p external uniformly distributed sound pressure acting on the panel

$p_D(x,y)$ amplitude of the sound pressure at the location (x,y,D) within the cavity

$P_{\max}$ maximum pressure

$P_{\min}$ minimum pressure

$\Delta\bar{p} = \dfrac{\int_0^a \int_0^b p - p_D \,\mathrm{d}x\,\mathrm{d}y}{ab} = p - \bar{p}_D$

t panel thickness

U and W numbers of the acoustic modes used in the x and y directions

w panel displacement

$v(x,y)$ panel velocity amplitude at (x,y)

$v_o(x,y)$ air particle velocity amplitude at the hole, which centre is located at (x,y)

$v_D(x,y,t)$ velocity at $z = -D$

$\bar{v} = \dfrac{\int_0^b \int_0^a v \,\mathrm{d}x\,\mathrm{d}y}{ab}$

$\bar{v}_D = \dfrac{\int_0^a \int_0^b \left[v + \dfrac{p - p_D}{\bar{Z}_o}\right] \mathrm{d}x\,\mathrm{d}y}{ab} =$ the average velocity at $z = -D$

$\bar{v}_o = \dfrac{\int_0^b \int_0^a v_o \,\mathrm{d}x\,\mathrm{d}y}{ab}$

$X_m(x)\,Y_n(y)$ (m,n) normal mode shape

Z impedance of the panel

$Z_a^{uw} = \mathrm{i}\rho_a\omega\dfrac{\coth(\mu^{uw}D)}{\mu^{uw}}$ acoustic impedance of the cavity

Z_o acoustic impedance of the hole

$\bar{Z}_o = \dfrac{Z_o}{\sigma}$ overall acoustic impedance of the open holes on the panel

$Z_{o,R}$ and $Z_{o,I}$ real and imaginary parts of Z_o

$Z_{mn} = \rho_p\dfrac{\mathrm{i}(\omega^2 - \omega_{mn}^2)}{\omega}$ modal impedance of the (m,n) mode of the panel without damping

$\nabla^4 = \left(\dfrac{\partial^2}{\partial x^2} + \dfrac{\partial^2}{\partial y^2}\right)^2$

$\bar{\alpha}$ = overall absorption coefficient

$\beta^{uw} = \int_0^a \int_0^b \cos\left(\dfrac{u\pi x}{a}\right)^2 \cos\left(\dfrac{w\pi y}{b}\right)^2 \mathrm{d}x\,\mathrm{d}y$

$\varepsilon_{mn} = \int_0^b \int_0^a X_m(x)\,Y_n(y)\,\mathrm{d}x\,\mathrm{d}y$

ϕ velocity potential function and ρ_a is the air density

$\gamma_{mn}^{uw} = \int_0^b \int_0^a \cos\left(\dfrac{u\pi x}{a}\right)\cos\left(\dfrac{w\pi y}{b}\right) X_m(x)\,Y_n(y)\,\mathrm{d}x\,\mathrm{d}y$

$\eta_{mn} = \int_0^b \int_0^a X_m(x)^2\,Y_n(y)^2\,\mathrm{d}x\,\mathrm{d}y$

$\lambda_m = m\pi/a$

$\lambda_n = n\pi/b$

$\mu^{uw} = \sqrt{\left(\dfrac{u\pi}{a}\right)^2 + \left(\dfrac{w\pi}{b}\right)^2 - \left(\dfrac{\omega}{c_a}\right)^2}$

ν the Poisson's ratio

ρ_p panel surface density

ω_{mn} resonant frequency of the (m,n) mode

1. Introduction

As micro-perforated panels and panel absorbers can be made of metal or plastic, their acoustic absorption performances are more long lasting than typical porous absorption materials. Besides, micro-perforated panels require small space to achieve high sound absorption when compared

with typical foam or porous materials. Acoustic theories for these two treatments were developed by Mulholland and Parbrook [1], Ford and McCormick [2], and Maa [3,4]. In Burgemeister and Hansen's recent work [5], perforated panels were used as a control source to achieve noise attenuation.

In many theoretical analyses of a micro-perforated panel backed by a cavity, the structural-acoustic cavity modes have not been focused on [3,4,6,7]. The coupling effects of the structural and acoustic cavity modes were studied experimentally and theoretically by Lyon [9], Pretlove [10], Guy [11], Dowell et al. [12], Oldham and Hillarby [13], and Pan [14,15]. In the absorption test of a micro-perforated panel conducted by Lee and Swenson [16], an additional sound absorption peak was unexpectedly found around the low-frequency range (50–100 Hz) due to the panel vibration effect. However, the study only focused on the absorption effect due to the perforations, and did not make use of the panel vibration effect to optimize the absorption bandwidth. Theoretical and experimental analyses of absorption due to panel vibrations were presented in the works of Ford and McCormic [2], Sakagami et al. [17], Frommhold et al. [18], and Sakagami et al. [19]. It was found that the sound absorption mechanism of a panel absorber was due to the panel/cavity resonance. These analyses, except for that of Ford and McCormic, neglected the bending stiffness of the panel. Kang and Fuchs [7] developed and experimentally verified a theory for micro-perforated membrane absorbers. They considered the vibration effect of the membrane but neglected the bending stiffness of the absorber. Takahashi and Tanaka [8] developed an absorption theory that considered an infinitely elastic perforated plate backed by a cavity. Therefore, there was no absorption peak due to the structural resonance in the predictions and experiments.

The objective of this paper is to develop a sound absorption formula for the combined effects of micro-perforated panel and panel absorbers using the modal analysis approach. A series of numerical cases shows the absorption performance of the acoustic treatment with the properties of the micro-perforated panel and panel absorber. Measurement results are used to verify the predictions.

2. Theory

2.1. Acoustical velocity potential

In Fig. 1, the boundary at $z = -D$ is flexible so that the panel can vibrate in typical mode shapes while the other walls are acoustically rigid. The acoustic velocity potential within the rectangular cavity is given by the following homogeneous wave equation [10]:

$$\nabla^2\phi - \frac{1}{c_a^2}\frac{\partial^2\phi}{\partial t^2} = 0, \tag{1}$$

where ϕ is the velocity potential function and c_a is the speed of sound.

The air particle velocities in the x, y, and z directions and pressures within the air cavity can be given by $\partial\phi/\partial x, \partial\phi/\partial y, \partial\phi/\partial z$, and $-\rho_a(\partial\phi/\partial t)$, respectively.

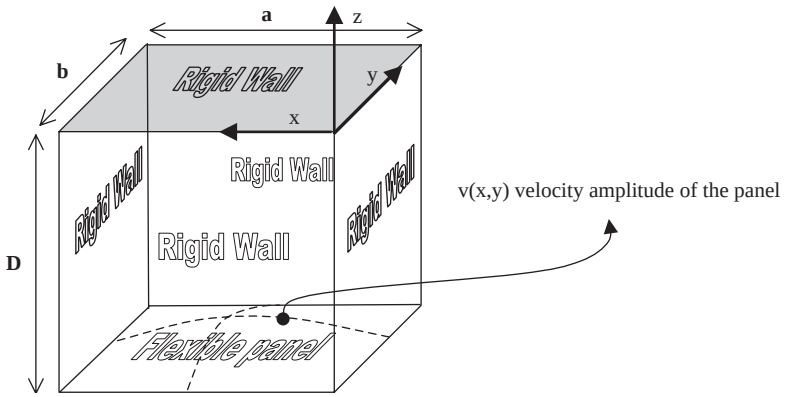

Fig. 1. Flexible perforated panel backed by a rectangular cavity.

The boundary conditions of the rectangular cavity to be satisfied are

$$\left.\frac{\partial\phi}{\partial x}\right|_{x=0} = \left.\frac{\partial\phi}{\partial x}\right|_{x=a} = 0, \quad \left.\frac{\partial\phi}{\partial y}\right|_{y=0} = \left.\frac{\partial\phi}{\partial y}\right|_{y=a} = 0, \tag{2a,b}$$

$$\left.\frac{\partial\phi}{\partial z}\right|_{z=0} = 0, \quad \left.\frac{\partial\phi}{\partial z}\right|_{z=-D} = v_D(x,y,t), \tag{2c,d}$$

where a and b are the length and width of the perforated panel, ρ_a is the air density, and $v_D(x,y,t)$ is the velocity at $z=-D$. If the panel is subject to a harmonic uniformly distributed sound pressure $pe^{i\omega t}$, then $v_D(x,y,t)$ can be expressed as $v_D(x,y)e^{i\omega t}$. In Fig. 2, the particle velocity at $z=-D$ is given by

$$v_D(x,y) = \begin{cases} v_o(x,y) & \text{for the areas of the holes,} \\ v(x,y) & \text{for the panel surface,} \end{cases} \tag{3}$$

where $v(x,y)$ is the panel velocity amplitude at (x,y) and $v_o(x,y)$ is the air particle velocity amplitude at the hole, the centre of which is located at (x,y). The air particle velocity amplitude is assumed to be constant within the area of each hole [8]. According to Maa [3,4] and Takahashi and Tanaka [8], the hole diameter of a micro-perforated plate and the perforation ratio should be from 0.05 to 1 mm, and 0.5 to 1.5%, respectively. As the viscous force at the air–structure interface in the hole depend on the relative velocity, the particle velocity at a hole on the panel is given by

$$Z_{o,R}(v_o(x,y) - v(x,y)) + Z_{o,I}v_o(x,y) = p - p_D(x,y), \tag{4}$$

where p is the external uniformly distributed sound pressure acting on the panel, $p_D(x,y)$ is the amplitude of the sound pressure at the location (x,y,D) within the cavity, Z_o is the acoustic impedance of the hole [3,4], and $Z_{o,R}$ and $Z_{o,I}$ are the real and imaginary parts of Z_o, as

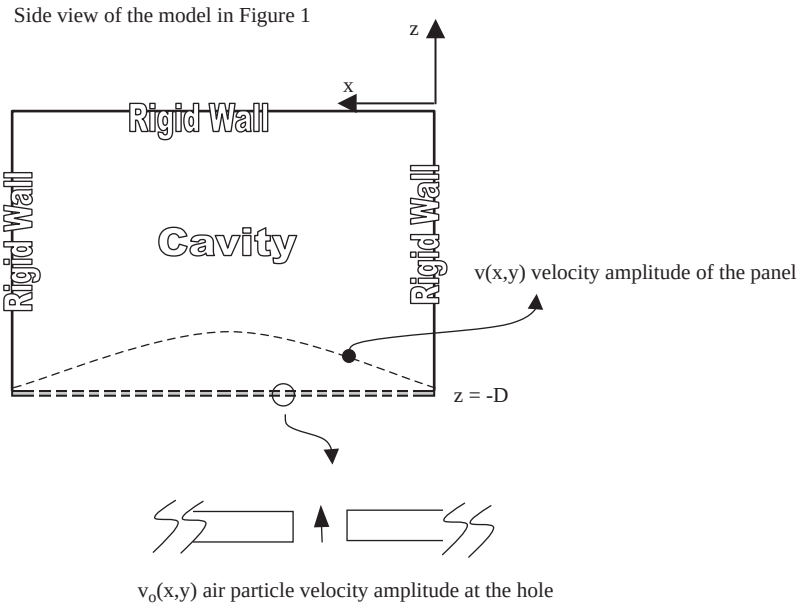

Fig. 2. Velocity amplitude of the perforated panel backed by a cavity.

given below

$$Z_{o,R} = \rho_a c_a \left(0.147 \frac{t}{d^2}\right) \left(\sqrt{9 + \frac{100 d^2 f}{32}} + 1.768 \sqrt{f} \frac{d^2}{t}\right), \tag{5a}$$

$$Z_{o,I} = \rho_a c_a 1.847 f t \left(1 + \frac{1}{\sqrt{9 + 50 d^2 f}} + 0.85 \frac{d}{t}\right), \tag{5b}$$

where f is frequency (kHz), t is the panel thickness, and d is the perforation diameter.

By applying the boundary conditions in Eqs. (2a, b), the solution of Eq. (1) can be expressed [10] as

$$\phi = \sum_{u=0}^{U} \sum_{w=0}^{W} [L^{uw} \cosh(\mu^{uw} z) + N^{uw} \sinh(\mu^{uw} z)] \cos\left(\frac{u\pi x}{a}\right) \cos\left(\frac{w\pi y}{b}\right) e^{i\omega t}, \tag{6}$$

where

$$\mu^{uw} = \sqrt{\left(\frac{u\pi}{a}\right)^2 + \left(\frac{w\pi}{b}\right)^2 - \left(\frac{\omega}{c_a}\right)^2},$$

U and W are the numbers of the acoustic modes used in the x and y directions, and L^{uw} and N^{uw} are coefficients that depend on the boundary conditions at $z = 0$ and $-D$.

Substituting Eq. (6) into Eqs. (2c,d) gives the following relations:

$$\left.\frac{\partial\phi}{\partial z}\right|_{z=0} = 0 \Rightarrow N^{uw} = 0, \tag{7a}$$

$$\left.\frac{\partial\phi}{\partial z}\right|_{z=D} = v_D e^{i\omega t} \Rightarrow L^{uw} = -\frac{\int_0^a \int_0^b v_D \cos\left(\frac{u\pi x}{a}\right)\cos\left(\frac{w\pi y}{b}\right) dx\,dy}{\beta^{uw}\mu^{uw}\sinh(\mu^{uw}D)}, \tag{7b}$$

where the perforation ratio σ is normally much less than 1. The integral in Eq. (7b) can be given by

$$\begin{aligned}
&\int_0^a \int_0^b v_D \cos\left(\frac{u\pi x}{a}\right)\cos\left(\frac{w\pi y}{b}\right) dx\,dy \\
&= \int_0^a \int_0^b \left[(1-\sigma)v + \sigma\frac{p - p_D + Z_{o,R}v}{Z_o}\right]\cos\left(\frac{u\pi x}{a}\right)\cos\left(\frac{w\pi y}{b}\right) dx\,dy \\
&\approx \int_0^a \int_0^b \left[v + \sigma\frac{p - p_D}{Z_o}\right]\cos\left(\frac{u\pi x}{a}\right)\cos\left(\frac{w\pi y}{b}\right) dx\,dy.
\end{aligned} \tag{8}$$

Consider the substitution of Eqs. (7b, 8) into Eq. (6). The pressure amplitude within the cavity at $z = -D$ can then be given by

$$\begin{aligned}
p_D = \sum_{u=0}^{U}\sum_{w=0}^{W}&\left[\frac{Z_a^{uw}}{\beta^{uw}}\int_0^a \int_0^b \left(v + \frac{p - p_D}{\bar{Z}_o}\right)\cos\left(\frac{u\pi x}{a}\right)\cos\left(\frac{w\pi y}{b}\right) dx\,dy\right] \\
&\times \cos\left(\frac{u\pi x}{a}\right)\cos\left(\frac{w\pi y}{b}\right),
\end{aligned} \tag{9}$$

where

$$\beta^{uw} = \int_0^a \int_0^b \cos\left(\frac{u\pi x}{a}\right)^2 \cos\left(\frac{w\pi y}{b}\right)^2 dx\,dy; \quad Z_a^{uw} = i\rho_a\omega\frac{\coth(\mu^{uw}D)}{\mu^{uw}}$$

is the acoustic impedance of the cavity. $\bar{Z}_o = Z_o/\sigma$ is the overall acoustic impedance of the open holes on the panel. The sound pressure p_D on the left-hand side of Eq. (9) is expressed in terms of itself. Thus, the terms in Eq. (9) must be rearranged.

$$\begin{aligned}
&\int_0^a \int_0^b p_D \cos\left(\frac{u\pi x}{a}\right)\cos\left(\frac{w\pi y}{b}\right) dx\,dy \\
&= \frac{\bar{Z}_o Z_a^{uw}}{\bar{Z}_o + Z_a^{uw}}\int_0^a \int_0^b \left[v + \frac{p}{\bar{Z}_o}\right]\cos\left(\frac{u\pi x}{a}\right)\cos\left(\frac{w\pi y}{b}\right) dx\,dy.
\end{aligned} \tag{10}$$

Substituting Eq. (10) into Eq. (9) gives the following equation:

$$\begin{aligned}
p_D = \sum_{u=0}^{U}\sum_{w=0}^{W}&\left[\frac{\bar{Z}_o Z_a^{uw}}{\beta^{uw}(\bar{Z}_o + Z_a^{uw})}\int_0^a \int_0^b \left(v + \frac{p}{\bar{Z}_o}\right)\cos\left(\frac{u\pi x}{a}\right)\cos\left(\frac{w\pi y}{b}\right) dx\,dy\right] \\
&\times \cos\left(\frac{u\pi x}{a}\right)\cos\left(\frac{w\pi y}{b}\right).
\end{aligned} \tag{11}$$

The integral

$$\int_0^a \int_0^b \cos\left(\frac{u\pi x}{a}\right)\cos\left(\frac{w\pi y}{b}\right)\mathrm{d}x\,\mathrm{d}y = 1 \text{ for } u = w = 0, \quad \text{otherwise } = 0.$$

2.2. Acoustic–structural interaction

Consider the governing equation for the vibration of the perforated panel subject to the external pressure p and internal pressure p_D at $z = -D$.

$$D_p\nabla^4 w(x,y,t) + \rho_p\frac{\partial^2 w(x,y,t)}{\partial t^2} = (p - p_D)\mathrm{e}^{\mathrm{i}\omega t}, \tag{12}$$

where

$$\nabla^4 = \left(\frac{\partial^2}{\partial x^2} + \frac{\partial^2}{\partial y^2}\right)^2; \quad D_p = \frac{Et^3}{12(1-v^2)}$$

is the panel's flexural rigidity, ρ_p is the panel surface density, E is Young's modulus, v is the Poisson ratio, w is the panel displacement which can be expressed as

$$w(x,y,t) = w(x,y)\mathrm{e}^{\mathrm{i}\omega t} = \sum_{m=1}^{M}\sum_{n=1}^{N} A_{mn}X_m(x)Y_n(y)\mathrm{e}^{\mathrm{i}\omega t}, \tag{13}$$

where A_{mn} is the modal amplitude of the (m,n) mode and $X_m(x)Y_n(y)$ is the (m,n) normal mode shape. M and N are the numbers of structural modes used. For a panel clamped at its two opposite sides and simply supported on the other two sides

$$X_m(x) = \sin(\lambda_m x), \tag{14a}$$

$$\begin{aligned} Y_n(y) = {} & \ell_{m,n}\sinh(\tilde{\lambda}_{m,n}y) - \tilde{\lambda}_{m,n}\sin(\ell_{m,n}y) \\ & - \frac{\ell_{m,n}\sinh(\tilde{\lambda}_{m,n}b) - \tilde{\lambda}_{m,n}\sin(\ell_{m,n}b)}{\cosh(\tilde{\lambda}_{m,n}b) - \sin(\ell_{m,n}b)}(\cosh(\tilde{\lambda}_{m,n}y) - \cos(\ell_{m,n}y)), \end{aligned} \tag{14b}$$

where $\lambda_m = m\pi/a$; $\ell_{m,n}$ and $\tilde{\lambda}_{m,n}$ are the nth for a particular m solution of the equation $\ell\tilde{\lambda}(\cos(\ell b)\cosh(\tilde{\lambda}b) - 1) + (\ell^2 - \tilde{\lambda}^2)\sin(\ell b)\sinh(\tilde{\lambda}b) = 0$ (see [20] for more details). For a panel simply supported,

$$X_m(x) = \sin(\lambda_m x),\ Y_n(y) = \sin(\lambda_n y), \tag{15a,b}$$

where $\lambda_m = m\pi/a$; $\lambda_n = n\pi/b$. (See Ref. [20] for the normal mode shapes of other boundary conditions.)

From Eq. (13), the velocity amplitude at the location (x,y) can be expressed in terms of the mode shapes $X_m(x)Y_n(y)$,

$$v(x,y) = \mathrm{i}\omega w(x,y) = \sum_{m=1}^{M}\sum_{n=1}^{N} B_{mn}X_m(x)Y_n(y), \tag{16}$$

where $B_{mn} = \mathrm{i}\omega A_{mn}$ is the modal velocity amplitude of the (m,n) mode.

Substituting Eqs. (11) and (16) into Eq. (12), multiplying $X_m(x)Y_n(y)$ on both sides, and taking the integration over the panel area give the following relation:

$$\eta_{mn}Z_{mn}B_{mn} - \sum_{m'=1}^{M}\sum_{n'=1}^{N}\sum_{u=0}^{U}\sum_{w=0}^{W}\frac{\gamma_{mn}^{uw}\gamma_{m'n'}^{uw}\bar{Z}_o Z_a^{uw}}{\beta^{uw}(\bar{Z}_o + Z_a^{uw})}B_{m'n'} = \frac{p\varepsilon_{mn}\bar{Z}_o}{(\bar{Z}_o + Z_a^{00})}, \tag{17}$$

where

$$\eta_{mn} = \int_0^b\int_0^a X_m(x)^2\,Y_n(y)^2\,\mathrm{d}x\,\mathrm{d}y; \gamma_{mn}^{uw} = \int_0^b\int_0^a \cos\left(\frac{u\pi x}{a}\right)\cos\left(\frac{w\pi y}{b}\right)X_m(x)\,Y_n(y)\,\mathrm{d}x\,\mathrm{d}y,$$

$$\varepsilon_{mn} = \int_0^b\int_0^a X_m(x)\,Y_n(y)\,\mathrm{d}x\,\mathrm{d}y,$$

where ω_{mn} is the resonant frequency of the (m,n) mode and

$$Z_{mn} = \rho_p\frac{\mathrm{i}(\omega^2 - \omega_{mn}^2)}{\omega}$$

is the modal impedance of the (m,n) mode of the panel without damping. If modal damping effects on the panel are considered, z_{mn} includes the modal damping ratio ξ_{mn} and can be rewritten as

$$Z_{mn} = \rho_p\frac{\xi_{mn}\omega_{mn}\omega + \mathrm{i}(\omega^2 - \omega_{mn}^2)}{\omega}. \tag{18}$$

From Eq. (17), a set of $M \times N$ equations that solve the $M \times N$ unknowns B_{mn} can be generated. Once the velocity amplitudes B_{mn} are known, the p_D and v in Eqs. (11) and (16) that are expressed in terms of B_{mn} can be found. The overall acoustic impedance $\bar{Z}$ and absorption coefficient $\bar{\alpha}$ [6] are defined as

$$\bar{Z} = \frac{p}{\rho_a c_a \bar{v}_D}, \quad \bar{\alpha} = \frac{4\mathrm{Re}(\bar{Z})}{(1 + \mathrm{Re}(\bar{Z}))^2 + (\mathrm{Im}(\bar{Z}))^2}, \tag{19a,b}$$

where

$$\bar{v}_D = \frac{\int_0^a\int_0^b\left[v + \dfrac{p - p_D}{\bar{Z}_o}\right]\mathrm{d}x\,\mathrm{d}y}{ab} = \text{the average velocity at } z = -D.$$

The impedance is normalized by $\rho_a c_a$.

2.3. Simplified approach

In the above section, the classical approach to obtain the absorption coefficient of the perforated panel backed by a cavity is quite lengthy. Hence, another approach to derive a simpler formula is introduced here. Consider the average velocities and pressure on both sides of Eq. (4) by taking integration over the panel area

$$Z_{o,R}(\bar{v}_o - \bar{v}) + Z_{o,I}\bar{v}_o = \Delta\bar{p}, \tag{20}$$

where

$$\Delta\bar{p} = \frac{\int_0^a \int_0^b p - p_D \,\mathrm{d}x\,\mathrm{d}y}{ab} = p - \bar{p}_D; \quad \bar{v} = \frac{\int_0^b \int_0^a v \,\mathrm{d}x\,\mathrm{d}y}{ab}; \quad \bar{v}_o = \frac{\int_0^b \int_0^a v_o \,\mathrm{d}x\,\mathrm{d}y}{ab}.$$

The average panel velocity $\bar{v}$ and average velocity at $z = -D$ can be given by

$$\bar{v} = \frac{\Delta\bar{p}}{Z}, \quad \bar{v}_D = (1-\sigma)\bar{v} + \sigma\bar{v}_o, \tag{21a,b}$$

where Z is the impedance of the panel. Now, replace $\Delta\bar{p}$ with $p - p_D$ in Eq. (12). Then the average velocity and impedance can be given by

$$\bar{v} = \sum_{m=1}^{M}\sum_{n=1}^{N} \frac{\Delta\bar{p}\varepsilon_{mn}\varepsilon'_{mn}}{\eta_{mn}Z_{mn}}, \quad Z = \frac{\Delta\bar{p}}{\bar{v}} = \left(\sum_{m=1}^{M}\sum_{n=1}^{N} \frac{\varepsilon_{mn}\varepsilon'_{mn}}{\eta_{mn}z_{mn}}\right)^{-1}. \tag{22a,b}$$

Substituting Eq. (21a) into Eq. (20) to eliminate $\Delta\bar{p}$ gives

$$\bar{v}_o = \frac{(Z + Z_{o,R})}{Z_o}\bar{v}. \tag{23}$$

Then, substituting Eq. (23) into Eq. (21b) to eliminate $\bar{v}_o$ gives

$$\bar{v}_D = \frac{\dfrac{Z_{o,R} + (1-\sigma)Z_{o,I}}{\sigma} + Z}{\bar{Z}_o}\bar{v} \approx \frac{\bar{Z}_o + Z}{\bar{Z}_o}\bar{v} \text{ when } \sigma \ll 1. \tag{24}$$

Here, the acoustic impedances of the perforated panel Z_p are defined in Eq. (25)

$$Z_p = \frac{\Delta\bar{p}}{\rho_a c_a \bar{v}_D}, \tag{25}$$

where the impedance in Eq. (25) is normalized by $\rho_a c_a$. Substituting Eqs. (21a, 24) into Eq. (25) gives

$$Z_p = \frac{\bar{Z}_o Z}{\rho_a c_a(\bar{Z}_o + Z)} = \frac{p - \bar{p}_D}{\rho_a c_a \bar{v}_D}. \tag{26}$$

Now, replace v_D with $\bar{v}_D$ in Eq. (7b) and substitute L^{uw} in Eq. (6). Then, $\bar{p}_D/\bar{v}_D$ in Eq. (26) can be given by

$$\bar{p}_D = Z_a^{00}\bar{v}_D \Rightarrow \frac{\bar{p}_D}{\rho_a c_a \bar{v}_D} = -\mathrm{i}\cot\left(\frac{\omega D}{c_a}\right). \tag{27}$$

By substituting Eq. (26) into Eq. (19a), the overall impedance and absorption coefficient of the perforated panel are then given by

$$\bar{Z}' = \frac{\bar{Z}_o Z}{\rho_a c_a(\bar{Z}_o + Z)} - \mathrm{i}\cot\left(\frac{\omega D}{c_a}\right), \quad \bar{\alpha}' = \frac{4\mathrm{Re}(\bar{Z}')}{(1 + \mathrm{Re}(\bar{Z}'))^2 + (\mathrm{Im}(\bar{Z}'))^2}. \tag{28a,b}$$

The overall impedance in Eq. (28a) is the same as that of the electro-acoustic analogy presented by Kang and Fuchs [7].

3. Theoretical results

Figs. 3a and b compare the absorption coefficients obtained from the two Eqs. (19b, 28b). In Fig. 3a, only the panel vibration effect is considered (i.e. not the micro-perforation effect). The predictions from the simplified approach are very close to those from the modal analysis solution for all frequencies, except at the frequencies around the second structural mode resonance (650 Hz) and the first acoustic mode resonance parallel to the panel surface (680 Hz). The simplified approach considers the average pressure and average panel velocity in Eqs. (20, 21a,b), which imply a uniformly distributed net pressure acting on the panel, and the panel vibrating like

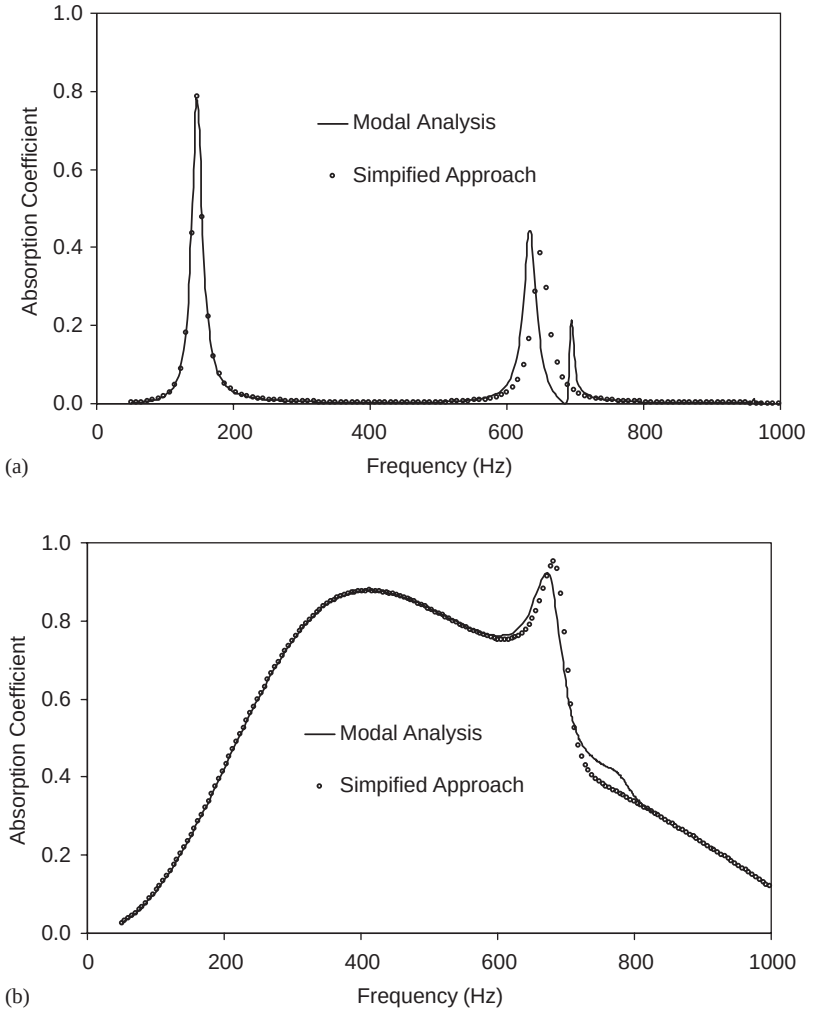

Fig. 3. (a) The absorption coefficients of a simply supported panel absorber predicted from the two approaches: $a = b = 0.5\,\text{m}$, $D = 150\,\text{mm}$, $\sigma = 0$, $\rho_p = 3\,\text{kg/m}^2$, $\xi = 0.04$, $\omega_{1\text{st}} = 2\pi \times 130$ radian, $\omega_{2\text{nd}} = 2\pi \times 650\,\text{rad}$. (b) The absorption coefficients of a simply supported micro-perforated absorber predicted from the two approaches: $a = b = 0.5\,\text{m}$, $D = 150\,\text{mm}$, $\sigma = 0.01$, $d = 0.4\,\text{mm}$, $t = 0.3\,\text{mm}$, $\rho_p = 1\,\text{kg/m}^2$, $\xi = 0.04$, $\omega_{1\text{st}} = 2\pi \times 700\,\text{rad/s}$.

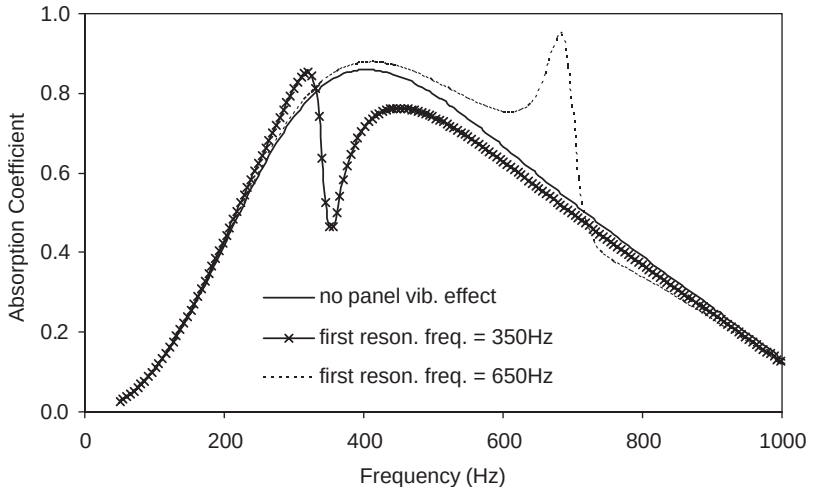

Fig. 4. The absorption coefficients of a simply supported micro-perforated absorber for different structural resonant frequencies; $a = b = 0.2\,\text{m}$, $D = 150\,\text{mm}$, $\sigma = 0.01$, $d = 0.4\,\text{mm}$, $t = 3\,\text{mm}$, $\rho_p = 1\,\text{kg/m}^2$.

a piston. In other words, only the (0,0) acoustic mode is considered in the wave equation, and the higher acoustic mode resonances parallel to the panel surface are neglected (i.e. the resonant peak of the higher acoustic mode disappears in Fig. 3a). The stiffness of the air cavity for the second structural mode is higher than that in the multi-mode approach. Thus, the resonant frequency of the second structural mode is higher. In Fig. 3b, both the panel vibration and micro-perforation effects are considered. The resonant frequencies of the higher structural modes are out of the frequency range studied (i.e. only the first structural mode is included). In this case, the effect of the first acoustic mode resonance (680 Hz) on the absorption is dimmed by the micro-perforation effect. It can be seen that the predictions from the simplified approach are almost the same as those from the modal analysis solution for all frequencies.

In Fig. 4, the first structural resonant frequencies of the cases with the panel vibration effect are 350 and 650 Hz, respectively. The absorption peak frequency of the micro-perforation effect is 400 Hz. The comparison of the cases with and without the panel vibration effect shows that if the forcing frequency is higher than the first structural resonant frequency (350 Hz for the crossed line, and 650 Hz for the dashed line), the structural vibration degrades the absorption performance. At this frequency range the panel vibrates in the direction of the air particle movements at the holes. The velocities of the air particles are lower than the panel vibration. Thus, the lower relative velocity causes lower sound absorption. In contrast if the forcing frequency is lower than the first structural resonant frequency, the structural vibration enhances the absorption performance. The panel vibrates in the direction opposite to that of the air particle movements. This occurs because of a phase change of 180° at the structural resonance. The velocities of the air particles relative to the panel vibration are higher. Thus, the higher relative velocity causes higher sound absorption. If the structural resonant frequency is higher than the absorption peak frequency caused by the perforations (see the dashed line in Fig. 4), the two peaks that are caused by the perforations and structural vibration are combined together to widen the effective absorption bandwidth.

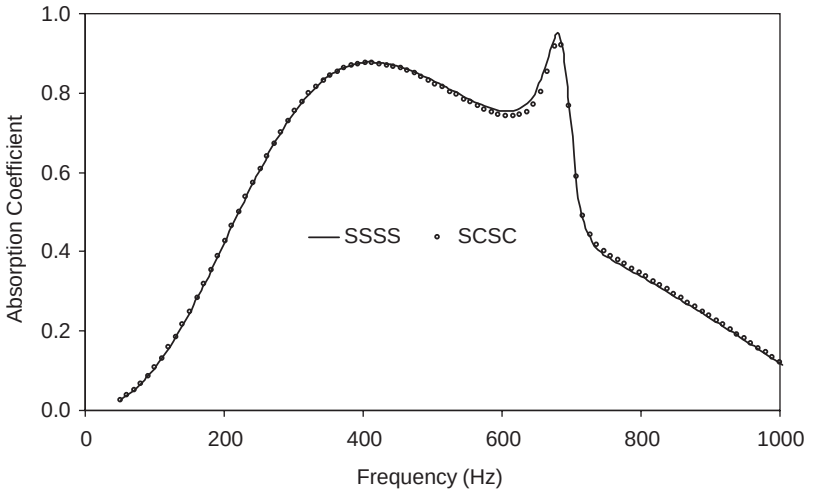

Fig. 5. The absorption coefficients of a micro-perforated absorber for different vibrating mode shapes; $a = b = 0.1\,\text{m}$, $D = 150\,\text{mm}$, $\sigma = 0.01$, $d = 0.4\,\text{mm}$, $t = 0.3\,\text{mm}$, $\rho_p = 1\,\text{kg/m}^2$, $\xi = 0.04$, $\omega_{1\text{st}} = 2\pi \times 700\,\text{rad/s}$.

Moreover, the negative effect caused by the panel vibration on the absorption performance is much less than that in the case of the structural resonant frequency lower than the absorption peak frequency (see the big trough on the crossed line at the structural resonant frequency).

Fig. 5 shows the absorption coefficients of a perforated absorber with the two different clamping conditions: two opposite sides simply supported and two opposite sides clamped (SCSC), and four sides simply supported (SSSS). The first structural resonant frequencies and other input parameters of the two cases are set to be equal. The resonant frequencies of the higher structural modes are out of the frequency range studied. In other words, the only difference in the two cases is the panel vibrating mode shape. It is obvious that the mode shape of the vibrating plate does not significantly affect the absorption.

Fig. 6 shows the effect of the structural damping on the absorption performance. The damping effect can improve the absorption performance at the frequencies between the structural resonant frequencies and the peak frequency of the micro-perforation effect, and decrease the peak absorption values of the structural resonances.

4. Experimental results

The experimental absorption results were obtained using the impedance tube and standing wave method (see Fig. 7 or [21] for the setup details). Fig. 7 shows the layout of the experiment. A small loudspeaker was placed at one end of the tube. The test material was placed at the other end. The sound field in the tube was the standing wave formed by the incident and reflected waves. The standing wave pressure ratio (the ratio of maximum root-mean square pressure to minimum root-mean square pressure) can be obtained by moving the probe microphone connected to a carriage

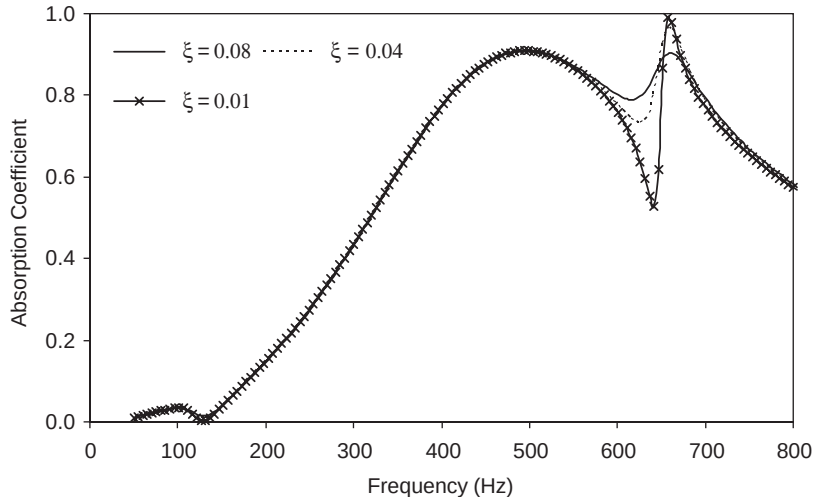

Fig. 6. The absorption coefficients of a simply supported micro-perforated absorber for different damping factors; $a = b = 0.2\,\text{m}$, $D = 40\,\text{mm}$, $\sigma = 0.01$, $d = 0.4\,\text{mm}$, $t = 2\,\text{mm}$, $\rho_p = 2\,\text{kg/m}^2$, $\omega_{1\text{st}} = 2\pi \times 130\,\text{rad/s}$, $\omega_{2\text{nd}} = 2\pi \times 650\,\text{rad/s}$.

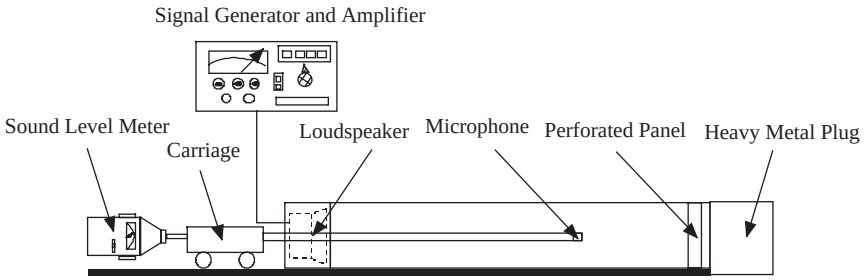

Fig. 7. The layout of the impedance tube.

along the tube. The absorption coefficient can be calculated by

$$\frac{4P_{\max}P_{\min}}{(P_{\max}+P_{\min})^2},$$

where $P_{\max}$ is the maximum pressure and $P_{\min}$ is the minimum pressure.

Figs. 8a–c and 9a–c show the comparisons between predicted and measured absorption coefficients for the two micro-perforated absorbers with $D = 20, 40, 80\,\text{mm}$. The prediction results are generated from Eq. (19b). The damping ratio is chosen as 0.04, and the mode shapes are assumed to be a summation of double sine functions. According to the experimental results in Figs. 8a–c, there is a peak or trough at 650 Hz, which is not significantly affected by the cavity depth, and it is believed that the peak is caused by the structural resonant frequency ω_{11}. Thus, the first structural resonant frequency ω_{11} in the predictions is selected as 650 Hz. Similarly, in Figs. 9a–c, the first and second structural resonant frequencies are selected as 280 and 1170 Hz,

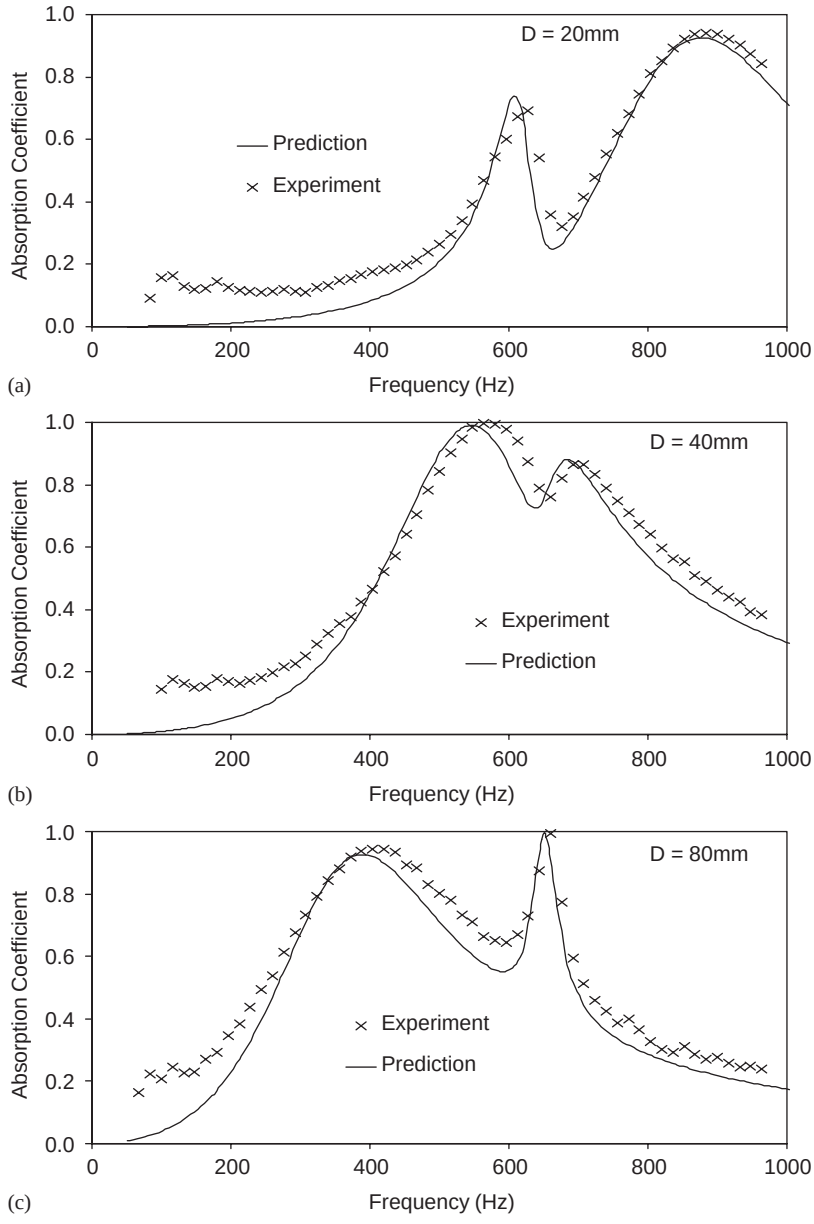

Fig. 8. The predicted and measured absorption coefficients of a single layer absorber with different cavity thicknesses; $a = b = 0.1\,\text{m}$, $\sigma = 0.005$, $d = 0.8\,\text{mm}$, $t = 3\,\text{mm}$, $\rho_p = 3\,\text{kg/m}^2$, $\xi = 0.04$, $\omega_{1\text{st}} = 2\pi \times 650\,\text{rad/s}$.

respectively. The agreements between the calculations and measurements are generally reasonable. The absorption peaks due to the structural resonances and the micro-perforation can be found in the two cases. The peaks due to the panel resonances can widen the absorption bandwidth by appropriately selecting parameters such as panel thickness, perforation diameter,

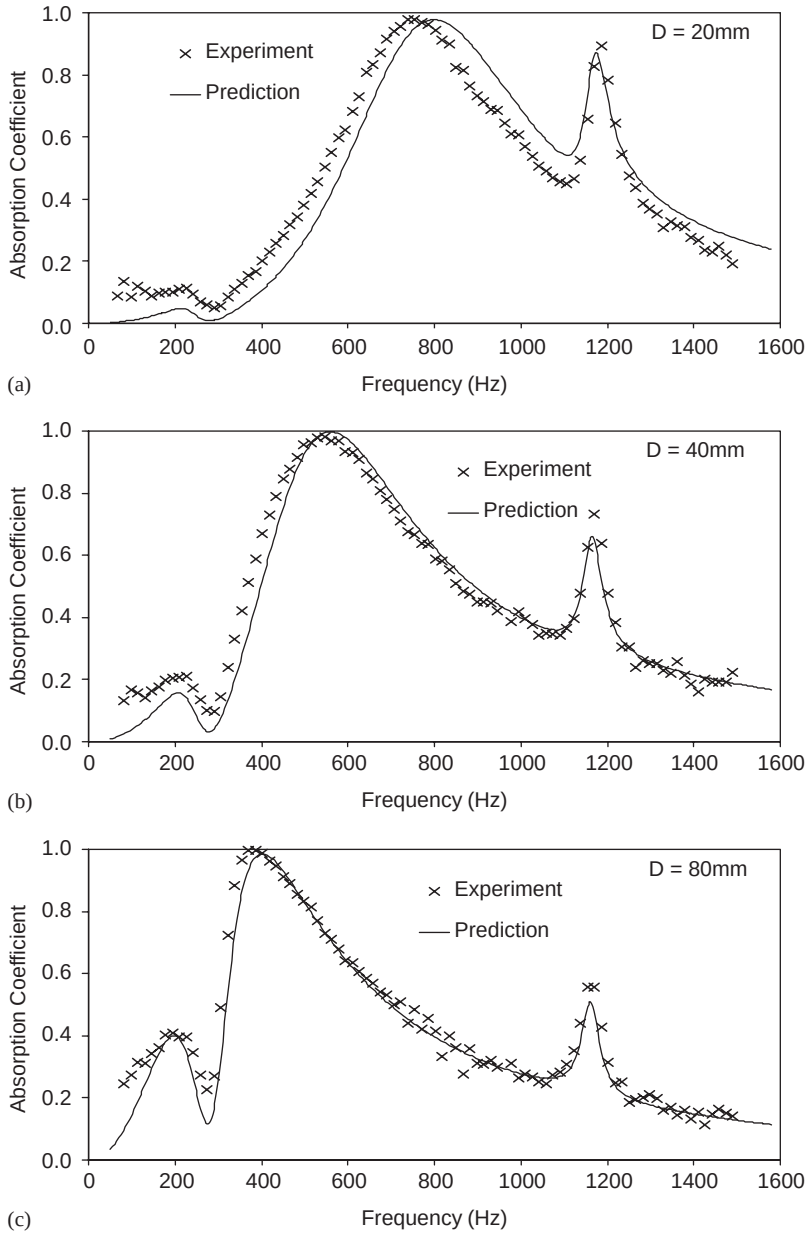

Fig. 9. The predicted and measured absorption coefficients of a single layer absorber with different cavity thicknesses; $a = b = 0.1\,\text{m}$, $\sigma = 0.005$, $d = 0.4\,\text{mm}$, $t = 0.8\,\text{mm}$, $\rho_p = 0.8\,\text{kg/m}^2$, $\xi = 0.04$, $\omega_{1\text{st}} = 2\pi \times 280\,\text{rad/s}$, $\omega_{2\text{nd}} = 2\pi \times 1170\,\text{rad/s}$.

and perforation spacing, etc. (see Figs. 8b–c), otherwise the panel vibration effect deteriorates the absorption performance at the structural resonant frequency (see the absorption coefficients around 280 Hz in Fig. 9c).

5. Conclusions

A theoretical model has been presented for predicting the absorption coefficient of a absorber, considering the two effects of micro-perforation and finite flexible panel vibration. The predictions for the absorbers show good agreement with the measurements. It can be concluded that (1) the absorption peak due to the panel vibration effect can widen the absorption bandwidth of a micro-perforated absorber by appropriately selecting parameters such as panel thickness, perforation diameter, and perforation spacing etc., such that the structural resonant frequency is higher than the absorption peak frequency that is caused by the perforations; (2) the comparison of the cases of different panel mode shapes does not show a significant difference in the absorption performance; and (3) the structural damping effect can improve the absorption performance at the frequencies between the structural resonant frequencies and the peak frequency of the micro-perforation effect, and decrease the peak absorption values of the structural resonances.

Acknowledgements

The work described in this paper was fully supported by a grant from the Research Grants Council of the Hong Kong Special Administrative Region, China [9040683 CityU 1032/02E].

References

[1] K.A. Mulholland, H.D. Parbrook, Transmission of sound through apertures of negligible thickness, *Journal of Sound and Vibration* 5 (3) (1967) 499–508.
[2] R.D. Ford, M.A. McCormick, Panel sound absorbers, *Journal of Sound and Vibration* 10 (3) (1969) 411–423.
[3] D. Maa, Microperforated panel wideband absorber, *Noise Control Engineering Journal* November–December (1987) 77–84.
[4] D. Maa, Potential of microperforated panel absorber, *Journal of Acoustical Society of America* 104 (5) (1998) 2861–2866.
[5] K.A. Burgemeister, C.H. Hansen, Reduction of radiated sound by use of actively controlled perforated panels, *International Journal of Active Control* 1 (1) (1995) 45–64.
[6] D. Takahashi, A new method for predicting the sound absorption of perforated absorber systems, *Applied Acoustics* 51 (1) (1997) 71–84.
[7] K. Kang, H.V. Fuchs, Predicting the absorption of open weave textiles and micro-perforated membranes backed by an air space, *Journal of Sound and Vibration* 220 (5) (1999) 920–950.
[8] D. Takahashi, M. Tanaka, Flexural vibration of perforated plates and porous elastic materials under acoustic loading, *Journal of the Acoustical Society of America* 112 (4) (2002) 1456–1464.
[9] R.H. Lyon, Noise reduction of rectangular enclosures with one flexible wall, *Journal of the Acoustical Society of America* 35 (1963) 1791–1797.
[10] A.J. Pretlove, Free vibrations of a rectangular panel backed by a closed rectangular cavity, *Journal of Sound and Vibration* 2 (3) (1965) 197–209.
[11] R.W. Guy, The transmission of sound through a cavity-backed finite plate, *Journal of Sound and Vibration* 27 (1973) 207–223.
[12] E.H. Dowell, G.F. Gorman, D.A. Smith, Acoustoelasticity: general theory acoustical natural modes and forced response to sinusoidal excitation including comparisons with experiment, *Journal of Sound and Vibration* 52 (1977) 519–542.

[13] D.J. Oldham, S.N. Hillarby, The acoustical performance of small close fitting enclosures—part 1: theoretical models, *Journal of Sound and Vibration* 150 (1991) 261–281.
[14] J. Pan, D.A. Bies, The effect of fluid-structural coupling on sound waves in an enclosure—theoretical part, *Journal of the Acoustical Society of America* 87 (2) (1990) 691–707.
[15] J. Pan, D.A. Bies, The effect of fluid-structural coupling on sound waves in an enclosure—experimental part, *Journal of the Acoustical Society of America* 87 (2) (1990) 708–717.
[16] J. Lee, G.W. Swenson, Compact sound absorbers for low frequencies, *Noise Control Engineering Journal* 38 (3) (1992) 109–117.
[17] K. Sakagami, D. Takahashi, H. Gen, M. Morimoto, Acoustic properties of an infinite elastic plate with a back cavity, *Acustica* 78 (1993) 288–295.
[18] W. Frommhold, H.V. Fuchs, S. Sheng, Acoustic performance of membrane absorbers, *Journal of Sound and Vibration* 170 (5) (1994) 621–636.
[19] K. Sakagami, M. Kiyama, M. Morimoto, D. Takahashi, Sound absorption of a cavity-backed membrane: a step towards design method for membrane-type absorbers, *Applied Acoustics* 49 (1996) 237–249.
[20] A.W. Leissa, *Vibration of Plates*, Scientific and Technical Information Division, Office of Technology Utilization, NASA, 1969.
[21] D.A. Bies, C.H. Hansen, *Engineering Noise Control: Theory and Practice*, second ed., Appendix D Absorption coefficients based upon impedance tube measurements, E & FN Spon, London, New York, 1996, pp. 521–525.